An unexpected role for brain-type sodium channels in coupling of cell surface depolarization to contraction in the heart

Sebastian K. G. Maier*, Ruth E. Westenbroek*, Kenneth A. Schenkman†, Eric O. Feigl‡, Todd Scheuer*, and William A. Catterall*§

Departments of *Pharmacology, †Pediatrics, and ‡Physiology and Biophysics, University of Washington, Seattle, WA 98195

Contributed by William A. Catterall, December 27, 2001

Voltage-gated sodium channels composed of pore-forming α and auxiliary β subunits are responsible for the rising phase of the action potential in cardiac muscle, but the functional roles of distinct sodium channel subtypes have not been clearly defined. Immunocytochemical studies show that the principal cardiac pore-forming α subunit isoform $Na_v1.5$ is preferentially localized in intercalated disks, whereas the brain α subunit isoforms $Na_v1.1$, $Na_v1.3$, and $Na_v1.6$ are localized in the transverse tubules. Sodium currents due to the highly tetrodotoxin (TTX)-sensitive brain isoforms in the transverse tubules are small and are detectable only after activation with β scorpion toxin. Nevertheless, they play an important role in coupling depolarization of the cell surface membrane to contraction, because low TTX concentrations reduce left ventricular function. Our results suggest that the principal cardiac isoform in the intercalated disks is primarily responsible for action potential conduction between cells and reveal an unexpected role for brain sodium channel isoforms in the transverse tubules in coupling electrical excitation to contraction in cardiac muscle.

Voltage-gated sodium channels are responsible for the initiation of action potentials in excitable cells. They are composed of a pore-forming α subunit and auxiliary β subunits (1). Ten genes encoding α subunits have been identified, and nine have been functionally expressed. These different isoforms have distinct patterns of development and localization in the nervous system, skeletal and cardiac muscle, and different pharmacological properties. Isoforms preferentially expressed in the central nervous system ($Na_v1.1$, 1.2, 1.3, and 1.6) are inhibited by nanomolar concentrations of tetrodotoxin (TTX), as is the isoform present in adult skeletal muscle ($Na_v1.4$). In contrast, the primary cardiac isoform ($Na_v1.5$) requires micromolar concentrations of TTX for inhibition because of the presence of a cysteine instead of an aromatic residue in the pore region (2). Sodium channel α subunits are associated with one or two auxiliary β subunits, $\beta1$, $\beta2$, or $\beta3$. These auxiliary subunits modulate channel gating, interact with extracellular matrix, and play a role as cell adhesion molecules (3, 4).

There is uncertainty about which α subunit isoforms are expressed in cardiac myocytes. mRNA for $Na_v1.5$, the primary cardiac isoform, and $Na_v1.1$, which is primarily expressed in the central nervous system, are both found in cardiac tissue (5). $Na_v1.1$ protein is expressed in the sino-atrial node in newborn rabbits (6) and in ventricular tissue (7). $Na_v1.2$, $Na_v1.3$, and $Na_v1.6$ are thought to be exclusively neuronal. $Na_v1.3$ is predominant in the early stages of development, whereas $Na_v1.2$ and $Na_v1.6$ are predominant in adult brain (8–13).

This study defines the sodium channel α subunits expressed in single ventricular myocytes and their role in cardiac physiology. Using specific antibodies, we show that $Na_v1.1$, $Na_v1.3$, $Na_v1.5$, and $Na_v1.6$ are differentially located within the ventricular myocyte. The brain isoforms $Na_v1.1$, $Na_v1.3$, and $Na_v1.6$ are present in the transverse tubular system, whereas the major cardiac isoform $Na_v1.5$ is present in the intercalated disks. $Na_v1.1$, $Na_v1.3$, and $Na_v1.6$ mediate small sodium currents in ventricular myocytes compared with $Na_v1.5$, but they contribute significantly to coupling of cell surface depolarization to contraction because of their location in the transverse tubules. Our results provide the first evidence, to our knowledge, for a unique functional role of TTX-sensitive brain-type sodium channels in the heart.

Methods

All procedures were approved by the Institutional Animal Care and Use Committee of the University of Washington.

Cell Isolation. Ventricular myocytes were isolated from adult male (8–10 weeks) wild-type B6129F1 mice, as described (14).

Antibodies. Anti-SP19 is directed against a conserved region of the intracellular loop between domains III and IV of the sodium channel α subunit and was characterized previously (15). Antibodies against $Na_v1.1$, $Na_v1.2$, and $Na_v1.3$ were purchased from Chemicon International (Temecula, CA; anti-RI, -RII, and -RIII) (13). The antibody recognizing $Na_v1.6$ (anti-Scn8a) came from Alomone Labs (Jerusalem). The antibody recognizing $Na_v1.5$ was generated against peptide SH1 (KTEPQAPGCGETPEDS), corresponding to residues 1122–1137 of the α subunit of $Na_v1.5$ (5). The specificity of anti-SH1 was demonstrated by immunoblotting (data not shown).

Immunocytochemistry. Single ventricular myocytes were plated on laminin-coated glass coverslips and incubated (5% CO_2, 37°C) for 6–12 h. Myocytes were fixed with 4% paraformaldehyde for 30 min, rinsed in 0.1 M phosphate, 0.1 M Tris buffer (TB), and in 0.1 M Tris-buffered saline (TBS), then blocked in 2% avidin-TBS and rinsed in TBS, then blocked in 2% biotin-TBS and rinsed in TBS. The myocytes were incubated with antibodies (diluted 1:15 in TBS containing 0.75% Triton X-100 and 1% normal goat serum) overnight at 4°C. Myocytes were then rinsed in TBS, incubated in biotinylated goat anti-rabbit IgG (diluted 1:300), and rinsed in TBS, incubated in avidin D fluorescein (diluted 1:300), rinsed in TBS, rinsed in TB, and rinsed in distilled water briefly. Coverslips were mounted on slides by using Vectashield (Vector). Cells were viewed by using a BioRad MRC 600 confocal microscope. For control sections, primary antibodies were preincubated with their antigenic peptide or no primary antibody was used.

Electrophysiology. Whole-cell cardiac sodium current (I_{Na}) was recorded at room temperature from rod-shaped, striated, and

Abbreviations: TTX, tetrodotoxin; n.s., not significant.

§To whom reprint requests should be addressed at: University of Washington, Department of Pharmacology, 1959 NE Pacific Street, Campus Box 357280, Seattle, WA 98195. E-mail: wcatt@u.washington.edu.

The publication costs of this article were defrayed in part by page charge payment. This article must therefore be hereby marked "*advertisement*" in accordance with 18 U.S.C. §1734 solely to indicate this fact.

Ca^{2+}-tolerant cells within 8 h of isolation. The low-sodium bath solution contained (in mM): 10 NaCl, 110 CsCl, 1.2 $MgCl_2$, 1.5 $CaCl_2$, 10 Hepes, 10 tetraethylammoniumchloride, 5.0 sucrose, 5.0 glucose, 5.0 $CoCl_2$, pH 7.4, with NaOH. The high-sodium bath solution contained 120 NaCl and no CsCl. The pipette solution contained: 124 Cs-aspartate, 1.0 NaCl, 2.0 $MgCl_2$, 10 Hepes, 10 EGTA, pH 7.3, with CsOH when used with the low-sodium extracellular solution; 5.0 NaCl and 120 Cs-aspartate were substituted when used with high-extracellular sodium.

Pipette resistance was 1–2 MΩ when filled with recording solution. Cell and electrode capacitance and series resistance (>85%) were compensated with internal voltage–clamp circuitry. Residual linear leak and capacitance were subtracted by using a P/4 protocol. Currents were recorded with an Axopatch 200 amplifier (Axon Instruments, Union City, CA), and data were collected and analyzed with PULSE (HEKA Electronics, Lambrecht/Pfalz, Germany) and IGOR (WaveMetrics, Lake Oswego, OR) software and presented as mean ± SE.

Working Heart Preparations

Guinea Pig. Isovolumic nonejecting working hearts were studied as described (16). Briefly, adult male guinea pigs were anesthetized, and the heart was surgically removed and mounted on a Langendorff apparatus for retrograde perfusion via the aorta. The perfusate contained (in mM): 118 NaCl, 4.7 KCl, 1.2 $MgSO_4$, 1.2 KH_2PO_4, 11 glucose, 2.0 CaCl, 2.0 pyruvate, and 25 $NaHCO_3$, supplemented with 5 units per liter of insulin and bubbled with 95% O_2 and 5% CO_2, 37°C. Perfusion pressure was 60 mmHg (1 mmHg = 133 Pa). To measure isovolumic left ventricular pressure, a latex balloon connected to a custom-made catheter tip pressure transducer (Millar Instruments, Houston, TX; 5.5F, no. SPR-783) was placed in the left ventricle. Hearts were paced at 240 beats per minute, and left ventricular end-diastolic pressure was kept constant at 8–10 mmHg. The difference between isovolumic diastolic and systolic pressures is reported as left ventricular developed pressure. The rate of left ventricular pressure development (the derivative of the pressure) and its maximum (dP/dt_{max}) are also reported.

Mouse. We used a simplified working heart preparation to confirm effects of TTX on cardiac contractility in the mouse. Animals were anaesthetized, hearts removed and mounted on a Langendorff apparatus, and perfused at 37°C retrogradely through a 16-G Teflon cannula in the aorta by using the buffer described for guinea pigs. Perfusion pressure was 75 mmHg. The heart was paced at 480 beats per minute. A catheter tip manometer (Millar, 1.4F) was inserted via the aortic cannula into the left ventricle, and intraventricular pressure was measured.

$Na_v1.1$-Expressing Mammalian Cells. Stable $Na_v1.1$-expressing HEK-293 cells, a generous gift from Glaxo Wellcome, were used to examine the properties of these channels (17). The same solutions and stimulation protocols as mentioned above were used for characterization of channel function and the action of CssIV.

Chemicals. β scorpion-toxin CssIV was a kind gift of Sandrine Cestèle and Marie-France Martin-Eauclaire. Biotinylated goat anti-rabbit IgG, avidin D fluorescein, avidin, biotin, Vectashield, and normal goat serum were purchased from Vector. All other chemicals were purchased from Sigma.

Results

Immunolocalization of $Na_v1.1$, $Na_v1.3$, $Na_v1.5$, and $Na_v1.6$ Channels in Single Cardiomyocytes. To examine whether brain-type sodium channel α subunits are present in ventricular cardiomyocytes and to determine their localization compared with the major cardiac isoform $Na_v1.5$, we incubated isolated adult mouse myocytes with an antibody that recognizes a sequence conserved in all sodium channel isoforms (anti-SP19) or with antibodies recognizing specific α subunit isoforms $Na_v1.1$ (anti-$Na_v1.1$), $Na_v1.2$ (anti-$Na_v1.2$), $Na_v1.3$ (anti-$Na_v1.3$), $Na_v1.5$ (anti-$Na_v1.5$), and $Na_v1.6$ (anti-$Na_v1.6$). Using the antibody recognizing all of these sodium channels, we observed sodium channel localization at high density at the regions of cell-to-cell contact, the intercalated disks (Fig. 1 *a* and *b*). Channel staining was also observed at lower density in a striated pattern (Fig. 1 *a* and *b*). Staining sections of ventricular tissue confirmed these localization patterns (data not shown). Interestingly, the α subunit isoforms have distinct localizations, as determined with isoform-specific antibodies (Fig. 1 *c–h*). Staining for the principal cardiac isoform ($Na_v1.5$, Fig. 1*c*) is very prominent at the cell margins, representing the area of the intercalated disks, with no detectable specific staining in the rest of the cell. This distinct localization was confirmed in ventricular tissue, where clustering of $Na_v1.5$ at the intercalated disks is very prominent (Fig 6, which is published as supporting information on the PNAS web site, www.pnas.org). This contrasts with staining for the brain-type isoforms $Na_v1.1$ (Fig. 1 *g* and *h*), $Na_v1.3$ (Fig. 1*e*) and $Na_v1.6$ (Fig. 1*d*), which are distributed in a striated pattern throughout the depth of the cell, as seen when focusing at different planes, on the surface of the myocyte ($Na_v1.1$, Fig. 1*g*) or within the cell ($Na_v1.1$, Fig. 1*h*; $Na_v1.3$, Fig. 1*e*, and $Na_v1.6$, Fig. 1*d*). This striated staining pattern is very similar to that of α actinin, a marker for cardiac muscle z-lines, in ventricular tissue (7) (data not shown). No specific staining was observed with a specific antibody directed against the isoform $Na_v1.2$ (Fig. 1*f*). Antibodies preabsorbed with peptides showed no specific signals (Fig. 7, which is published as supporting information on the PNAS web site). Combination of the staining pattern obtained with anti-$Na_v1.5$ with that obtained with antibodies against brain-type sodium channels leads to an image very similar to the staining pattern observed with the broad specificity sodium channel antibody (anti-SP19). Evidently, the image obtained with this antibody recognizing conserved sodium-channel sequences represents the sum of the images obtained with the isoform-specific antibodies against $Na_v1.1$, $Na_v1.3$, $Na_v1.5$, and $Na_v1.6$.

Properties of the Sodium Current in Ventricular Myocytes. To determine the properties of the total sodium current, I_{Na} was recorded with the whole-cell voltage–clamp configuration in single mouse cardiomyocytes with a decreased external sodium concentration of 10 mM to reduce series resistance errors. Cell capacitance, which correlates with membrane area, was 127 ± 13 pF, and I_{Na} density, which represents the ratio of I_{Na} amplitude to cell capacitance, was 61.6 ± 6.6 pA/pF (n = 14). Parameters for half-maximal I_{Na} activation and half-maximal inactivation after fitting the data to a Boltzmann equation were: $V_a = -26.2 \pm 1.1$ mV, $k = -5.8 \pm 0.1$ mV for activation (n = 14) and $V_h = -47.0 \pm 1.1$ mV, $k = 8.0 \pm 0.2$ mV for inactivation (n = 10) (Fig. 2*a*).

Next we characterized the sensitivity of I_{Na} to TTX, a specific sodium channel blocker that has approximately 100-fold higher affinity for brain $Na_v1.1$, $Na_v1.3$, and $NA_v1.6$ as opposed to cardiac $Na_v1.5$ channels. We determined the dose–response relation for the inhibition of I_{Na} by using a depolarizing pulse to 0 mV (Fig. 2*b*; 10 mM NaCl extracellular). This dose–response curve was well fit by a single-site Hill equation with an EC_{50} value for TTX of 679 nM. This value is lower than most reports of the TTX sensitivity of the cardiac sodium channel, which are generally in the micromolar range. It is known that TTX affinity depends on the external sodium concentration (18, 19). Our EC_{50} value is similar to previous recordings using low sodium concentrations (20). In addition, it is in agreement with the sensitivity of cardiac preparations to micromolar TTX, after correction for the effect of sodium concentration (18). These

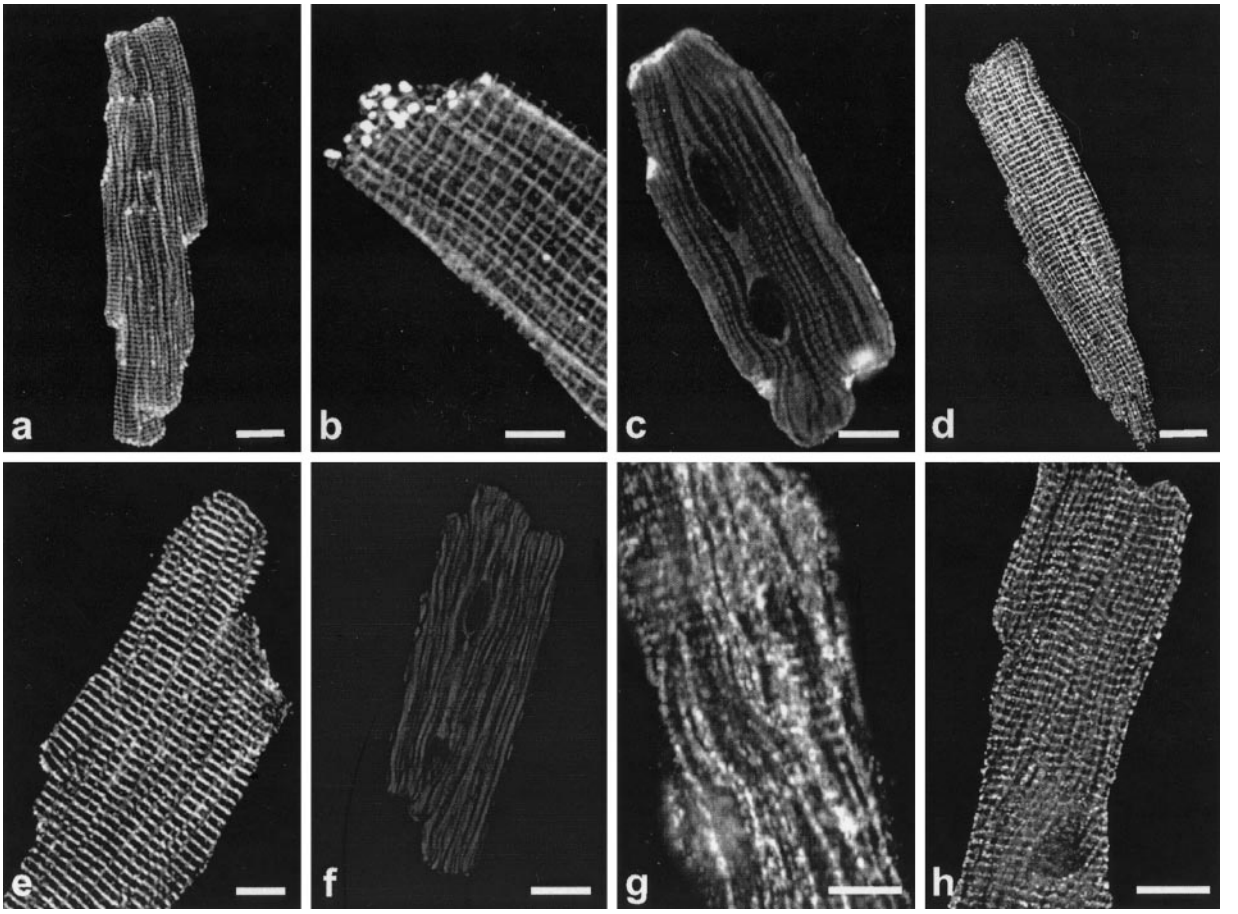

Fig. 1. Immunolocalization of sodium channel α subunits in single ventricular myocytes. (*a*) Single myocytes incubated with anti-SP19 recognizing conserved sodium channel sequences. Staining of the intercalated disks as well as weak striated staining of the transverse tubules is observed. (*b*) Close-up of a single myocyte stained with the same antibody, showing a striated pattern as well as clustered sodium channels at the end of the cell, the region of the intercalated disk. (*c*) Specific staining of intercalated disks along the cell margins for $Na_v1.5$. (*d–h*) Isoform-specific staining for brain-type sodium channels in ventricular myocytes. Specific striated staining pattern for $Na_v1.6$ (*d*), $Na_v1.3$ (*e*), and $Na_v1.1$ (*h*). The plane of focus was within the cell for these images. (*g*) Staining for $Na_v1.1$, focusing on the surface of the myocyte. (*f*) Specific antibodies directed against $Na_v1.2$ did not detect protein. The striated pattern shows that $Na_v1.1$, $Na_v1.3$, and $Na_v1.6$ are localized in the t-tubular system. Preabsorbed antibodies show no specific staining for $Na_v1.5$, $Na_v1.1$, $Na_v1.3$, and $Na_v1.6$, respectively (Fig. 7). (Bar = 10 μm.)

whole-cell voltage–clamp experiments indicate that $Na_v1.1$, $Na_v1.3$, and $Na_v1.6$ contribute at most a small fraction of I_{Na}, because low concentrations of TTX that would block these neuronal isoforms had no detectable effect.

Detection of I_{Na} Conducted by Brain-Type Sodium Channels After Treatment with the β Scorpion Toxin CssIV. The β scorpion toxin CssIV is a specific activator of neuronal sodium channels and does not activate the cardiac isoform (21). It negatively shifts the voltage dependence of activation of the rat neuronal $Na_v1.2$ channel but only after the channel is "primed" with a preceding depolarizing prepulse in the presence of toxin (21). β scorpion toxins have similar effects on $Na_v1.3$ (22). If it were also active on $Na_v1.1$ and $Na_v1.6$, CssIV could serve as a specific tool to reveal a low level of sodium current conducted by $Na_v1.1$, $Na_v1.3$, and $Na_v1.6$ in myocytes. We used a mammalian cell line stably transfected with $Na_v1.1$ (17) to examine whether CssIV also affects this channel. In high-sodium extracellular solution (120 mM), we measured the conductance–voltage relationship with and without a depolarizing prepulse in the presence of 1 μM CssIV. The peak sodium current density was 39.2 ± 7.5 pA/pF without prepulse and 64.0 ± 11.5 pA/pF with prepulse, representing an increase of 65.9 ± 23.9% caused by the preceding pulse (n = 8; Fig. 3). As previously described for $Na_v1.2$ (21), we observed a negative shift of the activation properties of $Na_v1.1$ after a depolarizing prepulse (Fig. 3). Fitting the activation curve without a prepulse to a Boltzmann equation, we obtained V_a = −10.5 ± 1.7 mV, k = −9.7 ± 0.8 mV. After the prepulse, the activation curve could not be fitted to a single Boltzmann equation, indicating the appearance of a fraction of channels with modified voltage dependence of activation. The negative shift in the activation curve with a prepulse results in substantial currents at potentials where none were present without a prepulse (Fig. 3 *Inset*). The negative shift of the activation curve and 65.9% increase of peak current are very similar to the effects of CssIV on $Na_v1.2$ expressed in tsA-201 cells (21). Because $Na_v1.1$, $Na_v1.2$, $Na_v1.3$, and $Na_v1.6$ are similar in amino acid sequence in the β scorpion toxin-binding region, it is expected that CssIV would affect $Na_v1.6$ similarly to the other brain-type sodium channel α subunit isoforms. Thus, CssIV is a useful tool for detecting brain-type sodium channels in cardiac myocytes.

Sodium currents in dissociated ventricular myocytes were measured in high-sodium extracellular solution during test pulses to −60 mV for 30 ms in control and in the presence of 1 μM CssIV (Fig. 4). In the absence of CssIV, little sodium current was elicited at this threshold test pulse potential (peak current: 1.0 ± 0.3 pA/pF, n = 6). In contrast, in the presence of CssIV with a depolarizing prepulse, a much larger current (peak

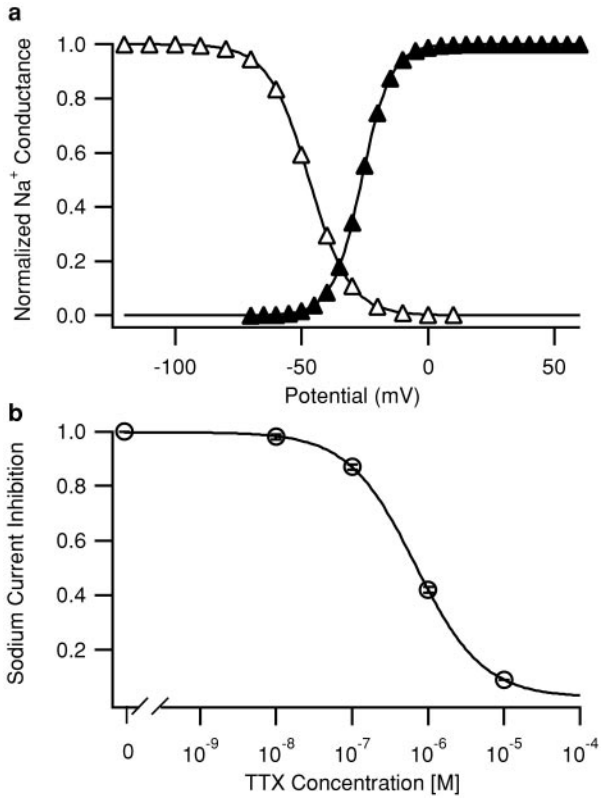

Fig. 2. Properties of the total cardiac sodium current in ventricular myocytes. (*a*) Mean sodium current activation (conductance versus voltage) curve (filled triangles) and steady-state inactivation curve (open triangles) in 10 mM extracellular NaCl. The voltage dependence of activation was determined by measuring the currents in response to 11-ms depolarizations to potentials from −70 mV to +60 mV in 5-mV steps from a holding potential of −100 mV. Depolarizations were applied once every 3.5 s. Peak inward current, *I*, during each depolarization was measured. Conductance, *g*, was calculated as $g = I/(V - V_{rev})$, where *V* was the depolarization potential, and V_{rev}, the measured reversal potential. Conductance was plotted as a function of test potential. Inactivation curves were generated by using 5-ms test pulses to 0 mV preceded by 50-ms depolarizations to the indicated potentials. Peak test pulse currents were measured and plotted as a function of prepulse potential. Conductance–voltage relationships or inactivation–voltage relationships from individual cells were fit with a Boltzmann function, $f(V) = 1/\{1 + \exp[(V - V_{.5})/k]\}$, where $V_{.5}$ is the half-activation (V_a) or half inactivation (V_h) voltage, and *k* is a slope factor. The curves shown were derived from the mean values of these fits as indicated in the text. (*b*) Concentration–response relationship for block of sodium current by TTX. EC_{50} = 679 nM (n = 2–13 for each concentration). Depolarizations to 0 mV from a holding potential of −100 mV were applied every 5 s, and peak sodium current was measured. Error bars represent SEM.

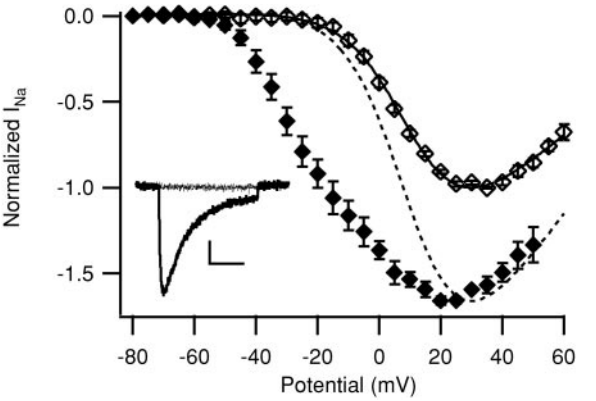

Fig. 3. Effect of β scorpion toxin CssIV on $Na_v1.1$ expressed in HEK 293 cells. Sodium currents due to stable expression of $Na_v1.1$ α subunits in HEK 293 cells were recorded by using high-sodium (120 mM) solutions. Mean normalized current–voltage relationships in the presence of 1 μM CssIV without a prepulse (open diamonds) or with a 2-ms prepulse to +50 mV preceding each depolarization (filled diamonds). All currents have been normalized to the peak of the current–voltage relationship without a prepulse. The solid line through the no-prepulse points is a fit of $I_{normalized} = (V - V_{rev})/\{1 + \exp[(V - V_a)/k]\}$ to the data. The dotted line is this fit normalized to the peak of the data obtained with a prepulse to show the negative shift in activation caused by the prepulse in the presence of CssIV. A 60-ms interval at the holding potential of −100 mV separated the prepulse from the test pulse. (*Inset*) Sodium currents obtained in response to depolarizations to −30 mV without (dotted) and with (solid) a prepulse in the presence of 1 μ M CssIV (Bar = 100 pA, 10 ms.)

current: 17.3 ± 6.2 pA/pF, $P = 0.008$ vs. no CssIV, unpaired Student's *t* test, $n = 5$) was recorded. A low concentration of TTX (181 nM) substantially reduced this CssIV-sensitive component of I_{Na} (2.7 ± 0.6 pA/pF, $P = 0.006$ vs. CssIV, $n = 8$). This 89.8% reduction of the CssIV-sensitive sodium current by 181 nM TTX indicates an EC_{50} for TTX of 20.6 nM, assuming one-to-one binding. This EC_{50} value is markedly lower than that typically reported in cardiac preparations (23–25) and similar to that reported for $Na_v1.1$ (9.6 nM TTX, 26), $Na_v1.3$ (1.8 nM TTX, 22), and $Na_v1.6$ (2.5 nM TTX, 17) when expressed in *Xenopus* oocytes or cell lines. Therefore, this CssIV-sensitive current is likely to be conducted by $Na_v1.1$, $Na_v1.3$, and $Na_v1.6$.

Role of Brain-Type Sodium Channels in Cardiac Contractility in Mouse and Guinea Pig Hearts. Our immunocytochemical data showed preferential localization of the neuronal isoforms, $Na_v1.1$, $Na_v1.3$, and $Na_v1.6$ in the t-tubular system. This location suggests that these channels may be necessary for rapid conduction of the action potential along the t-tubules into the interior of the cardiac cell to initiate synchronous contraction, thereby influencing ventricular performance and force generation. To test this hypothesis, we administered 100 or 200 nM TTX to isolated working mouse and guinea pig hearts. These TTX concentrations are expected to block 83 and 91% of neuronal sodium channels, respectively (assuming an EC_{50} of 20.6 nM) and have little effect on the cardiac $Na_v1.5$ isoform (1.5 and 3% block for 100 and 200 nM, respectively, assuming an EC_{50} of 6.3 μM in 122 mM sodium concentration (25). Thus, these TTX concentrations should isolate physiological effects of neuronal $Na_v1.1$, $Na_v1.3$, and $Na_v1.6$ from those of cardiac $Na_v1.5$ sodium channels. To assess the effects on contractile function, we measured left ventricular developed pressure (DP) and dP/dt_{max}, which cor-

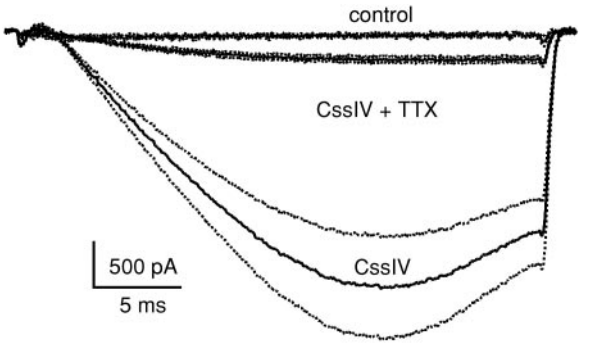

Fig. 4. Effect of TTX on sodium current in ventricular myocytes in the presence of 1 μM β scorpion toxin CssIV. Sodium currents were evoked with a 30-ms test pulse to −60 mV, without and with a 2-ms prepulse to +50 mV in high sodium (120 mM) saline. Mean traces obtained in the absence of a prepulse or CssIV (control, $n = 5$), with a prepulse in the presence of 1 μM CssIV (CssIV, $n = 6$), or with a prepulse in the presence of CssIV and 181 nM TTX (CssIV + TTX, $n = 8$). The dotted lines flanking each trace represent ± SEM.

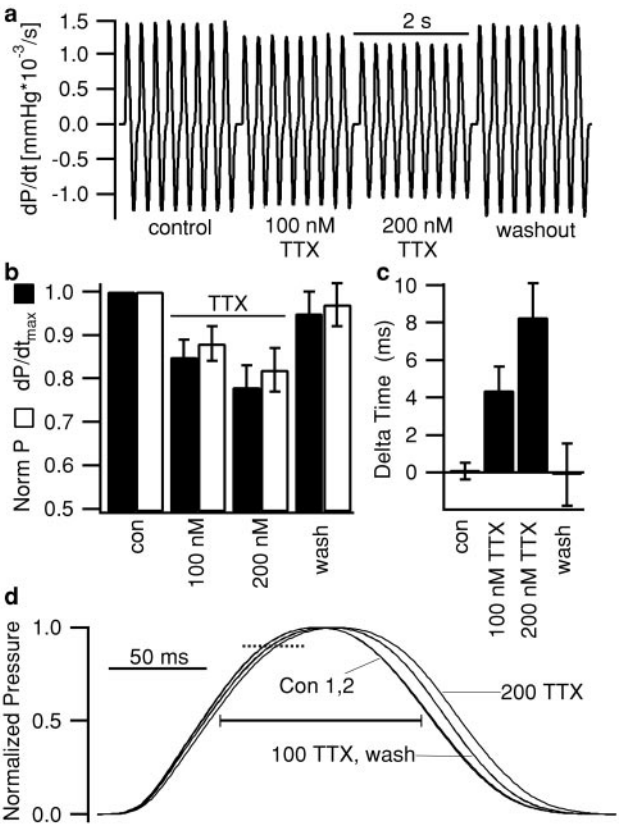

Fig. 5. Effect of TTX on myocardial contractility in isolated working guinea pig hearts. (*a*) Representative tracing of left ventricular isovolumic contractile performance (dP/dt) from a guinea pig heart under control conditions, in the presence of 100 or 200 nM TTX and after washout ($n = 4$). (*b*) Fractional change in maximal rate of left ventricular pressure development (dP/dt_{max}, ■) and in left ventricular developed pressure (P, □) caused by TTX relative to control conditions ($n = 4$). (*c*) Difference in mean time from stimulus to 90% of peak pressure compared with control [Delta time; see dotted line (*d*), $n = 7$]. This measure varied by 0.1 ± 0.4 ms (n.s.) between two control periods but increased by 4.4 ± 1.2 ms ($P < 0.01$ vs. control) and 8.3 ± 1.8 ms ($P < 0.001$) in 100 and 200 nM TTX, respectively. Washing reversed TTX effects (−0.1 ± 1.7 ms vs. control; n.s.). (*d*) Mean pressure traces obtained during two control periods (Con 1,2), in the presence of 100 or 200 nM TTX and after washout of TTX from a representative experiment where each trace was rescaled to match the control amplitude. Each mean trace was constructed from 10 consecutive beats. In the same experiments, the duration of systole at 50% of peak pressure (solid bar) increased from 117.8 ± 2.4 ms in control to 122.3 ± 2.4 ms ($P < 0.01$) and 126.5 ± 2.4 ms ($P < 0.01$) in 100 and 200 nM TTX, respectively, and was reversed on TTX washout (119.6 ± 1.4 ms, n.s., $n = 7$). Cycle length was maintained constant at 250 ms. Error bars represent ± SEM.

relates with basal contractility and is highly sensitive to acute changes (27). In mouse, TTX reduced dP/dt_{max} by 18.0% ($n = 3$, 100 nM TTX) and 31.7% ($n = 2$, 200 nM TTX), and the effect was reversible (data not shown). We performed more extensive experiments using an established guinea pig experimental model (16). In these experiments, 100 nM TTX decreased left ventricular dP/dt_{max} by 15 ± 4% ($P = 0.015$, paired Student's t test; Fig. 5 *a* and *b*) and left ventricular DP by 12 ± 4% ($P = 0.018$, $n = 4$, Fig. 5*c*). For 200 nM TTX, dP/dt_{max} was reduced by 22 ± 5% ($P = 0.006$) and DP by 18 ± 5% ($P = 0.012$). Washing out TTX caused almost complete recovery [$dP/dt_{max} = 95 \pm 5\%$; DP = 97 ± 5% of control; $n = 4$, not significant (n.s.), Fig. 5 *a* and *b*]. In addition, the development of left ventricular pressure was delayed after the pacing stimulus (Fig. 5 *c* and *d*), and the duration of systole was prolonged by TTX (Fig. 5*d*). The decreased contractility, delay in pressure development, and prolongation of systole can all be explained by a loss of synchrony of cardiac contraction. This indicates that brain-type sodium channels ($Na_v1.1$, $Na_v1.3$, and $Na_v1.6$) in the t-tubules are involved in linking depolarization of the cell surface to contraction in cardiac muscle.

Discussion

Differential Localization of Sodium Channel α Subunits in Cardiac Myocytes. Nine different sodium channel subtypes have been identified, but their functional role in heart has not been characterized fully. We determined the localization of sodium channel α subunits in isolated adult mouse ventricular myocytes. Our results demonstrate differential localization of four α subunit isoforms: $Na_v1.5$ is preferentially located at the intercalated discs, whereas $Na_v1.1$, $Na_v1.3$, and $Na_v1.6$ are found at the z-lines within the t-tubular system.

Our immunocytochemical results have both similarities to and important differences from previous reports. They agree with Malhotra *et al.*, who found $Na_v1.1$ in t-tubules in sections of mouse heart (7). Cohen reported intense labeling of $Na_v1.5$ at terminal intercalated discs, as we have found, but also observed labeling for $Na_v1.5$ along the cell surface and at the z-lines in adult rat ventricular tissue (28). A BLAST search of the amino acid sequence used to generate the anti-$Na_v1.5$ antibodies used in that study suggests that the antibodies would have also recognized $Na_v1.3$. In contrast, the sequence of the anti-$Na_v1.5$ antibody used in the present study is not expected to recognize brain channels. This was confirmed by transfecting tsA-201 cells with $Na_v1.1$ and $Na_v1.5$ and showing that the antibodies we used (anti-$Na_v1.1$, anti-$Na_v1.2$, anti-$Na_v1.3$, anti-$Na_v1.5$, and anti-$Na_v1.6$) were specific for their target proteins by immunocytochemistry. Therefore, it seems likely that the staining previously reported for $Na_v1.5$ (28) described the sum of the distributions of two sodium channel isoforms in cardiac tissue: $Na_v1.3$ and $Na_v1.5$. Our own data, together with the data of Cohen (28), allow us to conclude that $Na_v1.5$ is located at the intercalated disks and $Na_v1.1$, $Na_v1.3$, and $Na_v1.6$ in the t-tubular system. Our more specific antibodies highlight the sharply complementary distributions of the sodium channel α subunit isoforms in cardiac myocytes.

Functional Significance of Localization of $Na_v1.5$ Channels in Cardiac Myocytes. The clustering of $Na_v1.5$ at the intercalated discs and its high expression level relative to $Na_v1.1$, $Na_v1.3$, and $Na_v1.6$ suggest that the $Na_v1.5$ channels are specialized for the initiation of the action potential as it jumps from cell to cell. This high density of sodium channels is reminiscent of nodes of Ranvier in myelinated nerves, where depolarization jumps in saltatory fashion from node to node, and the intermediate internodal membrane is depolarized electrotonically. Our results raise the possibility that the action potential may jump from one end of the cell to the other end via $Na_v1.5$ channels, depolarizing the intervening cell surface membrane electrotonically. This architecture would allow the rapid propagation of the action potential through the working ventricular myocardium that is needed for proper function. If this form of conduction is correct for the surface membrane of cardiac myocytes, how is the action potential conducted rapidly and synchronously into the interior of the myocyte where calcium release activates the contractile proteins?

Functional Role of Sodium Currents Conducted by $Na_v1.1$, $Na_v1.3$, and $Na_v1.6$. Our results provide, to our knowledge, the first detection of sodium currents through brain-type $Na_v1.1$, $Na_v1.3$, and $Na_v1.6$ channels in ventricular myocytes. No TTX-sensitive sodium current characteristic of $Na_v1.1$, $Na_v1.3$, and $Na_v1.6$ is detected under standard recording conditions. TTX-sensitive sodium current was revealed when myocytes were treated with

β scorpion toxin to isolate current through $Na_v1.1$, $Na_v1.3$, and $Na_v1.6$ channels. That current was blocked with high affinity by TTX (EC_{50} = 20.6 nM). In the absence of β scorpion toxin, we estimate that a reduction in sodium current >5% in the presence of low TTX concentrations would have been detected. Because no reduction was observed, this represents an upper limit on the percentage of current due to TTX-sensitive isoforms. Thus, despite showing the presence of TTX-sensitive sodium channels using β scorpion toxin, our results parallel previous findings reporting an EC_{50} for TTX in the micromolar range in cardiac preparations and failing to detect a high-affinity population of sodium channels (19, 25, 29, 30).

Although the sodium current conducted by $Na_v1.1$, $Na_v1.3$, and $Na_v1.6$ channels is small, the specific t-tubular location of these channels suggests an important function. Calcium is released synchronously throughout the ventricular myocyte, and release begins within 2 ms of depolarization (31). This is in sharp contrast to tissues lacking t-tubules, such as atrial myocytes or Purkinje fibers, in which contraction is initiated at the periphery and propagates inward (32, 33). Thus, transverse tubules are necessary for the rapid propagation of the action potential into the center of the ventricular myocyte. Neuronal sodium channels may underlie this rapid conduction and excitation of the cell interior. Our observation that low TTX concentrations reduce cardiac contractility and desynchronize excitation–contraction coupling support the unexpected conclusion that brain-type sodium channels rapidly conduct the action potential along the t-tubules into the center of the myocyte, depolarizing the t-tubules, activating L-type calcium channels, and initiating excitation–contraction coupling.

Overall, our results give insights into the localization of sodium channel isoforms in cardiac tissue and suggest complementary physiological roles for these channels: $Na_v1.5$ in initiation and conduction of the cardiac action potential and $Na_v1.1$, $Na_v1.3$, and $Na_v1.6$ in coupling of cell surface depolarization to contraction. These data provide physiological evidence that TTX-sensitive brain-type sodium channels play an important role in action potential propagation in the myocyte and in excitation–contraction coupling.

We thank Dr. Sandrine Cestèle for helpful discussions, Dr. Marie-France Martin-Eauclaire for purifying the β scorpion toxin (Centre National de la Recherche Scientifique, Unité Mixte de Recherche 6560, Université de la Mediterranée, Marseille, France), and Thuy Vien and Wayne A. Ciesielski (University of Washington) for excellent technical assistance. This work was supported by Fellowship Ma 2252/1-1 from the Deutsche Forschungsgemeinschaft (to S.M.) and by National Institutes of Health Research Grant P01 HL44948 (to W.A.C.).

1. Catterall, W. A. (2000) *Neuron* **26,** 13–25.
2. Goldin, A. L. (2001) *Annu. Rev. Physiol.* **63,** 871–894.
3. Isom, L. L., De Jongh, K. S. & Catterall, W. A. (1994) *Neuron* **12,** 1183–1194.
4. Isom, L. L. (2001) *Neuroscientist* **7,** 42–54.
5. Rogart, R. B., Cribbs, L. L., Muglia, L. K., Kephart, D. D. & Kaiser, M. W. (1989) *Proc. Natl. Acad. Sci. USA* **86,** 8170–8174.
6. Baruscotti, M., Westenbroek, R., Catterall, W. A., DiFrancesco, D. & Robinson, R. B. (1997) *J. Physiol. (London)* **498,** 641–648.
7. Malhotra, J. D., Chen, C., Rivolta, I., Abriel, H., Malhotra, R., Mattei, L. N., Brosius, F. C., Kass, R. S. & Isom, L. L. (2001) *Circulation* **103,** 1303–1310.
8. Felts, P. A., Yokoyama, S., Dib-Hajj, S., Black, J. A. & Waxman, S. G. (1997) *Mol. Brain Res.* **45,** 71–82.
9. Beckh, S., Noda, M., Lübbert, H. & Numa, S. (1989) *EMBO J.* **8,** 3611–3616.
10. Noda, M., Ikeda, T., Suzuki, T., Takeshima, H., Takahashi, T., Kuno, M. & Numa, S. (1986) *Nature (London)* **322,** 826–828.
11. Suzuki, H., Beckh, S., Kubo, H., Yahagi, N., Ishida, H., Kayano, T., Noda, M. & Numa, S. (1988) *FEBS Lett.* **228,** 195–200.
12. Krzemien, D. M., Schaller, K. L., Levinson, S. R. & Caldwell, J. H. (2000) *J. Comp. Neurol.* **420,** 70–83.
13. Gordon, D., Merrick, D., Auld, V., Dunn, R., Goldin, A. L., Davidson, N. & Catterall, W. A. (1987) *Proc. Natl. Acad. Sci. USA* **84,** 8682–8686.
14. Guo, W., Xu, H., London, B. & Nerbonne, J. M. (1999) *J. Physiol. (London)* **521,** 587–599.
15. Gordon, D., Merrick, D., Wollner, D. A. & Catterall, W. A. (1988) *Biochemistry* **27,** 7032–7038.
16. Schenkman, K. A. & Yan, S. (2000) *Crit. Care Med.* **28,** 172–177.
17. Clare, J. J., Tate, S. N., Nobbs, M. & Romanos, M. A. (2000) *Drug Discov. Today* **5,** 506–520.
18. Reed, J. K. & Raftery, M. A. (1976) *Biochemistry* **15,** 944–953.
19. Doyle, D. D., Guo, Y., Lustig, S. L., Satin, J., Rogart, R. B. & Fozzard, H. A. (1993) *J. Gen. Physiol.* **101,** 153–182.
20. Arreola, J., Spires, S. & Begenisich, T. (1993) *J. Physiol. (London)* **472,** 289–303.
21. Cestèle, S., Qu, Y., Rogers, J. C., Rochat, H., Scheuer, T. & Catterall, W. A. (1998) *Neuron* **21,** 919–931.
22. Joho, R. H., Moorman, J. R., VanDongen, A. M. J., Kirsch, G. E., Silberberg, H., Schuster, G. & Brown, A. M. (1990) *Mol. Brain Res.* **7,** 105–113.
23. Cohen, C. J., Bean, B. P., Colatsky, T. J. & Tsien, R. W. (1981) *J. Gen. Physiol.* **78,** 383–411.
24. Satin, J., Kyle, J. W., Chen, M., Bell, P., Cribbs, L. L., Fozzard, H. A. & Rogart, R. B. (1992) *Science* **256,** 1202–1205.
25. Antoni, H., Bocker, D. & Eickhorn, R. (1988) *J. Physiol. (London)* **406,** 199–213.
26. Smith, R. D. & Goldin, A. L. (1998) *J. Neurosci.* **18,** 811–820.
27. Little, W. C. (1985) *Circ. Res.* **56,** 808–815.
28. Cohen, S. A. (1996) *Circulation* **94,** 3083–3086.
29. Muramatsu, H., Zou, A. R., Berkowitz, G. A. & Nathan, R. D. (1996) *Am. J. Physiol.* **270,** H2108–H2119.
30. Guo, X., Uehara, A., Ravindra, A., Bryant, S., Hall, S. & Moczydlowski, E. (1987) *Biochemistry* **26,** 7546–7556.
31. Cheng, H., Cannell, M. B. & Lederer, W. J. (1994) *Pflügers Arch.* **428,** 415–417.
32. Huser, J., Lipsius, S. L. & Blatter, L. A. (1996) *J. Physiol. (London)* **494,** 641–651.
33. Cordeiro, J. M., Spitzer, K. W., Giles, W. R., Ershler, P. E., Cannell, M. B. & Bridge, J. H. (2001) *J. Physiol. (London)* **531,** 301–314.